

# An RFID-enabled Inkjet-printed Soil Moisture Sensor on Paper for "Smart" Agricultural Applications

Sangkil Kim<sup>†</sup>, Taolan Le and Manos M. Tentzeris  
School of Electrical and Computer Engineering  
Georgia Institute of Technology  
Atlanta, GA, USA  
<sup>†</sup>ksangkil3@gatech.edu

Amal Harrabi  
Faculty of Science, Mathematics  
Physics and Natural of Tunis  
Tunisia

Ana Collado and Apostolos Georgiadis<sup>‡</sup>  
Centre Tecnologic de Telecomunicacions de Catalunya  
Catalunya, Spain  
ageorgiadis@cttc.es

**Abstract**—In this paper, an RFID-enabled inkjet-printed passive soil moisture sensor on paper for agricultural applications is presented and the design procedure, the operation principle and benchmarking experimental results are discussed in detail. A prototype made of a passive RFID tag integrated with a capacitive sensor, which consists of a printed interdigitated capacitor (IDC), has been printed on a low-cost paper substrate. The capacitance variation of the IDC shifts the resonant frequency of the RFID tag taking advantage of the soil-moisture based load matching variations since a matching condition changes due to the capacitive sensor. The proposed sensor can be easily integrated with conventional RFID systems for practical large-scale agricultural applications.

**Keywords**—inkjet printing; RFID-enabled sensor; soil moisture sensor; paper electronics

## I. INTRODUCTION

Due to the dwindling water resources around the world, one of the most critical issues of modern agriculture is to develop a high-efficiency, low-cost water control and management system [1]. Pervasive computing and advanced sensor technology have implemented robust sensor networks for agriculture applications but it has been challenging to deploy wireless system over large agricultural areas due to cost, environmental, and technical issues [2].

RFID-enabled sensor topologies have demonstrated significant advantages in the past [3-5], featuring a simple structure, low-cost implementation and compatibility with conventional wireless sensor networks (WSN) and RFID infrastructure [3]. Additive large-area fabrication processes, such as inkjet printing [4], can be easily used for mass production of low-cost RFID-enabled sensors, while low-power wireless sensor system implementations can be

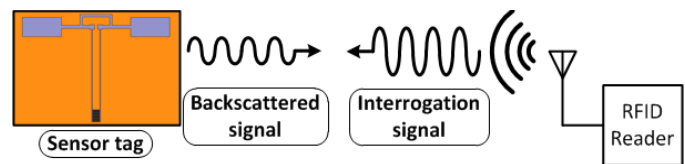


Fig. 1. Operation principle of the proposed RFID-enabled soil moisture sensor.

realized through the use of passive/semi-active RFIDs. The use of paper substrates has further enhanced the advantages of the printing technologies for agricultural applications since they are among the most eco-friendly and low-cost materials.

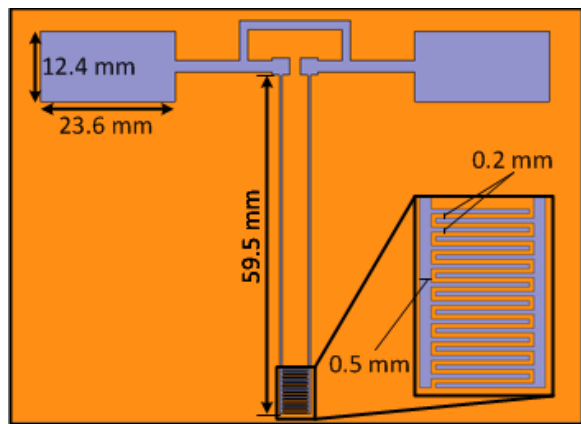
In this work, a novel inkjet-printed passive RFID-enabled soil moisture sensor is introduced, that utilizes a capacitive sensor for the detection of the soil moisture content. The design process and the measurement results are also presented in detail.

## II. RFID-ENABLED SENSOR TAG DESIGN

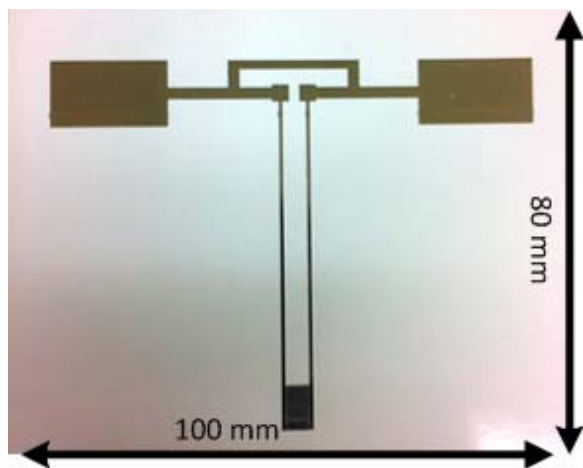
### A. Operation Principle

The operation principle of the proposed RFID-enabled soil moisture sensor is depicted in Fig. 1. This sensor responds to the reader when it collects enough power from the reader's interrogation signal to activate the RFID chip, which then sends out its own ID to the reader (backscattered signal) at the UHF RFID frequency band (915 MHz) following the EPC Gen 2 protocol. The magnitude of the backscattered signal is a function of the delivered power to the RFID chip. A capacitive sensor consisting of an interdigitated capacitor (IDC) is integrated with an RFID-tag to modify the the magnitude of the delivered power to the RFID chip depending on the moisture-based variable "load" material on the capacitive sensor. The resonant frequency (optimum

The work of S. Kim, T. Le and M. Tentzeris was supported by National Science Foundation (NSF). The work of A. Collado and Georgiadis was supported by EU Marie Curie FP7-PEOPLE-2009-IAPP 251557 and by the Spanish Ministry of Economy and Competitiveness project TEC 2012-39143



(a)



(b)

Fig. 2. (a) Geometry of the designed RFID-enabled sensor and (b) inkjet-printed sensor on paper.

matching frequency) of the dipole antenna shifts to lower values when the IDC sensor features higher capacitance values due to high-dielectric load materials (high moisture values). The electrical properties of the load (“moisture”) materials, such as the dielectric constant ( $\epsilon_r$ ) on the RFID-enabled sensor can be easily detected by observing the magnitude of the backscattered signal at the operation frequency, and thus the required minimum Tx (reader) power to activate the RFID chip, which can be easily recorded from since the reader. In this paper, the reader’s minimum required transmitted power to activate the RFID-enabled sensor was monitored since it is directly related to the magnitude of the backscattered signal as well as it is easy to record from the reader.

### B. RFID-Enabled Sensor Tag with A Capacitive Sensor

The geometry of the designed RFID-enabled capacitive sensor prototype is shown in Fig. 2(a). The IDC was printed at the end of electrodes to increase the sensor’s sensitivity as shown in the inset of Fig. 2(a), (b). The length of the electrodes was chosen to minimize the effect of soil to maintain the omni-directional radiation pattern. The IDC consisted of 20 fingers with a width of 200  $\mu\text{m}$ . The number of IDC’s fingers was chosen to optimize the sensor’s sensitivity

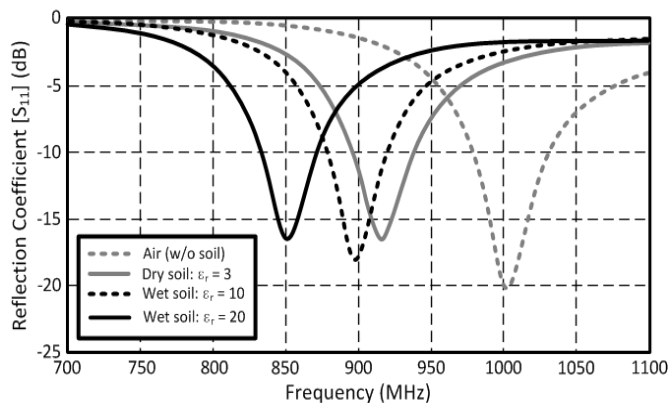


Fig. 3. Simulated reflection coefficients ( $S_{11}$ ) of the proposed soil moisture sensor in air, dry soil and wet soil.

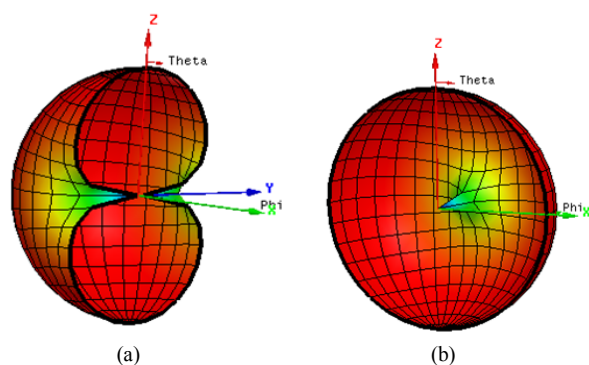


Fig. 4. Simulated radiation patterns on (a) E-plane (YZ-plane) and (b) H-plane (XZ-plane) at 915 MHz in free space.

while minimizing the effect on the antenna performance, such as the radiation pattern, due to the capacitive load. The gap between the fingers was also 200  $\mu\text{m}$  due to printing resolution on paper. The printable resolution is 50  $\mu\text{m}$  but 200  $\mu\text{m}$  resolution has been chosen in order to compensate possible fabrication errors, such as the nozzle malfunctioning and the ink spreading after printing on paper. The electrodes integrated with the IDC were connected in parallel to a passive RFID chip in order to optimize the sensitivity of the sensor resulted in the distance between the two electrodes (length of the IDC’s finger) of 4.3 mm. The antenna was designed based on the half-wavelength ( $\lambda_0/2$ ) dipole antenna. The rectangular termination patches which introduce additional inductance were placed to miniaturize the antenna. The length of the proposed antenna was 88 mm which was only 0.27  $\lambda_0$  (54 % of the length of half-wavelength dipole antenna) while the length of the half-wavelength dipole antenna is 164 mm. A T-matching network was utilized to match the designed sensor-enabled RFID antenna to a passive RFID chip at the operation frequency of 915 MHz. The used chip model was NXP’s SL3ICS1002/1202 chip and its impedance at 915 MHz was modeled 13.3 – j122  $\Omega$ . The RFID chip was modeled as a parallel resistor-capacitor (R-C) network to model the frequency dependence of the input impedance of the chip. The modeled resistor value (R) was 1.13 k $\Omega$  and the capacitance value (C) was 1.41 pF at 915 MHz. The inkjet-printed RFID-enabled sensor tag prototype on paper is shown in Fig. 2(b).

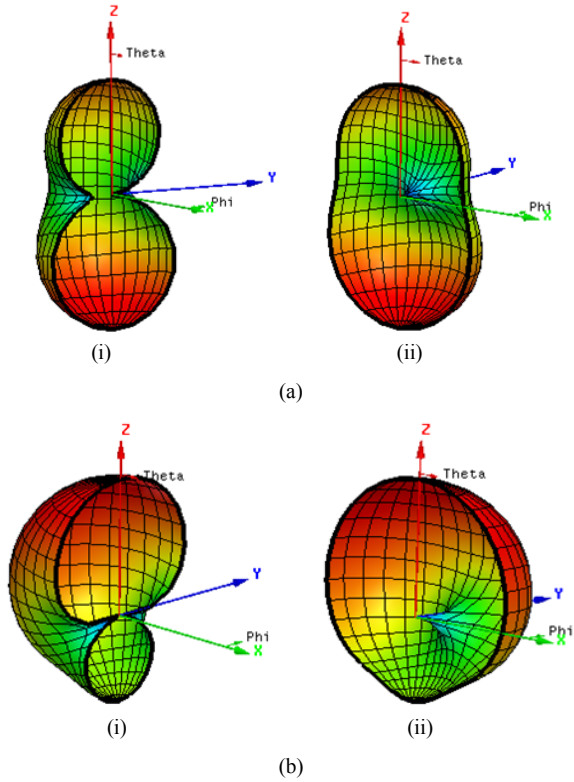


Fig. 5. Simulated radiation patterns on (i) E-plane (YZ-plane) and (ii) H-plane (XZ-plane) at the resonant frequency in (a) dry soil and (b) wet soil (water content: 20 %).

The simulated reflection coefficients values ( $S_{11}$ ) depending on the soil moisture content are shown in Fig. 3. The 3D full wave simulator ANSYS HFSS v11.1 was utilized to design the sensor tag. The proposed sensor tag had the resonant frequency at 1 GHz in free space, and it shifted to 915 MHz when the sensor tag was inserted in the dry soil. Only the IDC was completely buried in the soil. The resonant frequency of the simulated sensor tag on the modeled soil kept shifting to lower frequencies as the soil got more water content. The dried soil was modeled as a dielectric material which has a dielectric constant ( $\epsilon_r$ ) of 3.0 and loss tangent ( $\tan \delta$ ) of 0.01 [6]. The heavily wet soil which has the soil moisture content of 20 % was modeled as a high loss material with a poor conductivity ( $\sigma$ ) value of 0.15 S/m and high dielectric constant ( $\epsilon_r$ ) of 20 [6]. The lightly wet soil which has the soil moisture content of 5 % ( $\epsilon_r$ : 10,  $\sigma$ : 0.06) was also studied to confirm the shift of the resonant frequency depending on the electrical properties of the soil.

The simulated radiation patterns on E-plane (YZ-plane) and H-plane (XZ-plane) at 915 MHz are shown in Fig. 4 and Fig. 5. The sensor tag has an omni-directional radiation pattern in the free space. The sensor tag in the dry/wet soil has also omni-directional radiation patterns despite the high dielectric constant and loss. The calculated total gain values of the antenna in the free space, the dry soil and the wet soil at each resonant frequency are 1.11 dBi, 1.26 dBi, and 0.56 dBi, respectively.

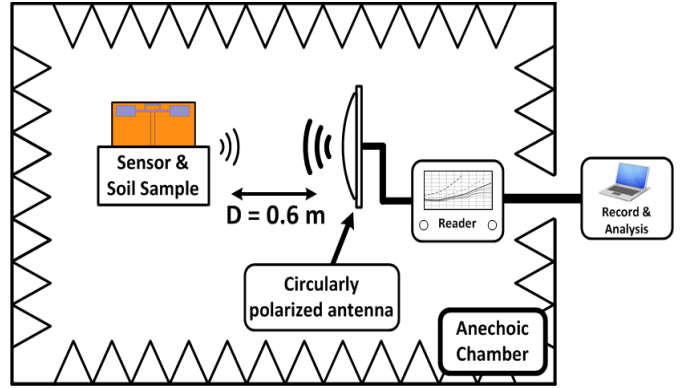


Fig. 6. RFID-enabled sensor measurement setup.

### C. RFID-enabled Sensor Tag Fabrication

The designed RFID-enabled sensor was inkjet-printed on photo paper. Kodak photo paper was used as substrate and its thickness was 228.6  $\mu\text{m}$  (9 mils). The electrical properties of the photo paper were reported in [7]. The reported relative dielectric constant ( $\epsilon_r$ ) was 2.9 and loss tangent ( $\tan \delta$ ) was 0.045 at 915 MHz. The paper has a relatively high  $\tan \delta$  due to its cellulose-based composition but it is not a critical parameter for the RF applications on thin substrate, such as the RFID antenna and a slot antenna, because E-field has a weak interaction with the lossy paper substrate [4,7]. Paper is also sensitive to ambient moisture due to its high water absorption rate which increases the sensitivity of the paper-based moisture sensor.

The Dimatix DMP2800 inkjet printer, and the Dimatix 10 pL cartridge (DMC-11610) were utilized to print the silver nanoparticle ink on paper. The angle of the printer head was set to 4.5° to print a pattern in a drop spacing of 20  $\mu\text{m}$  resulting in a print resolution of 1270 dpi (dots per inch). DGP 40LT-15C ink from ANP was used for the fabrication in this work. The printed sensor tag was sintered at 130 °C for 2 hours in a thermal oven to burn off the solvent to make it conductive. The reported printed silver nanoparticle ink after the thermal sintering process has a DC conductivity in the range of  $9 \times 10^6$  S/m  $\sim 1.1 \times 10^7$  S/m with roughness of about 11 ~ 15 nm [4,7]. The conductivity value is about 14.3 ~ 17.5 % of a conductivity value of bulk silver ( $6.3 \times 10^7$  S/m), and similar to the bulk iron ( $1.0 \times 10^7$  S/m).

## III. EXPERIMENTAL RESULTS

### A. Soil Sample Preparation

Garden soil was prepared for the wireless measurement in this work. It was baked in a thermal oven at 100 °C for 2 hours to remove soil moisture completely, and its weight after drying process was 355.3 g. The dried soil sample was put in an acrylic box whose size was 85 mm  $\times$  130 mm  $\times$  52 mm (width  $\times$  length  $\times$  height). The moisture content of soil can be calculated from (1) [8], and distilled water was prepared to increase the soil moisture content ( $u$ ) regularly.

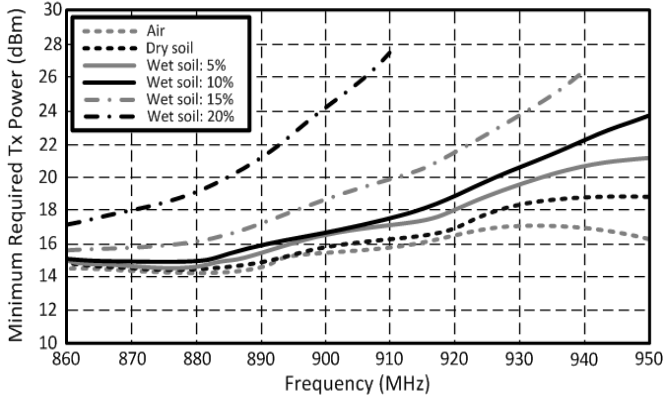


Fig. 7. Measured minimum required transmitting (Tx) power to activate the RFID-enabled sensor depending on soil moisture content.

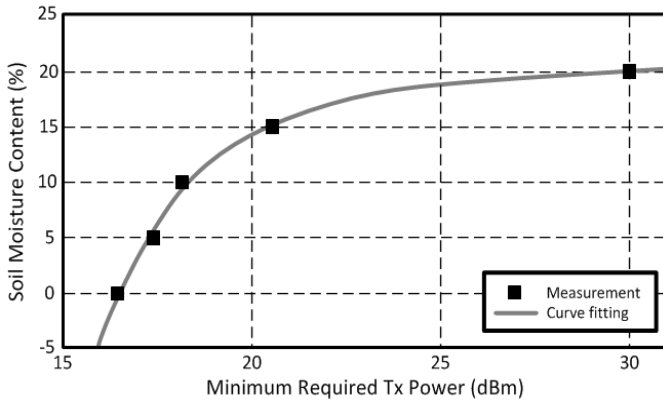


Fig. 8. Mapping the measured minimum required transmitting (Tx) power variation depending on soil moisture content at 915 MHz.

$$u = \frac{m_{wet} - m_{dry}}{m_{dry}} \times 100 \quad (1)$$

Where:  $m_{wet}$  and  $m_{dry}$  are the mass of the wet soil and the dry soil, respectively. The weight of each prepared water sample was 17.8 g, and it was set to increase the soil moisture content linearly by 5 %.

### B. Sensor Measurement

The fabricated sensor tag was buried in the prepared dry soil, and its wireless performance was comprehensively tested. About 8 mm of the sensor tag was buried in the dried soil sample to cover the capacitive sensor (interdigitated capacitor) completely. The prepared sensor tag and the soil sample was measured in an anechoic chamber as shown in Fig. 6. The distance between the sensor tag and a reader antenna was 60 cm. The reader antenna is a circularly polarized panel antenna which has a gain of 8 dBi. The Voyantic Tagformance reader was used for the measurements. The minimum required transmitted (Tx) power to activate the RFID chip was recorded at different frequencies in the 860 MHz ~ 950 MHz bandwidth.

The measured minimum required Tx power depending on soil moisture is shown in Fig. 7. The soil moisture content was increased by 5 % regularly, and the minimum required

Tx power was measured. It was clearly observed that the minimum required Tx power was increased over the frequency range as the soil moisture content increased. Fig. 8 shows a fitted curve of the measured required Tx power to the soil moisture content at 915 MHz. The measured data was fitted to an exponential function as shown in (2) where  $x$  is the minimum required Tx power in dBm. The root-mean-square error (RMSE) of the fitted curve was only 1.3.

$$U = 15.81e^{\frac{7.946x}{1000}} - 1.454 \times 10^4 e^{-0.4072x} \quad (2)$$

The soil moisture content ( $U$ ) can be extracted by mapping the measured minimum required Tx power through (2). The wet soil was dried at 100 °C for 2 hours to verify the weight of the soil after the measurement. It weighted 353.3 g after the drying process compared to 355.3 g before the beginning of the measurements which presented an error of 0.56 % which can be negligible.

## IV. CONCLUSION

A novel inkjet-printed passive RFID-enabled soil moisture sensor on paper has been demonstrated for the first time. A step-by-step design procedure has been discussed in detail, and the performance of the design sensor tag has been experimentally demonstrated. The sensor demonstrated shift of the minimum required Tx power level due to the soil moisture variation. The measured data was fitted to the mapping curve to extract the soil water content. Numerous agricultural applications can be stemmed from this work, such as a water level sensor or a rain fall sensor. The next step of this work is to build a robust reader system and improve the RFID-enabled sensor tag sensitivity.

## REFERENCES

- [1] T. Wark, P. Corke, P. Sikka, L. Klingbeil, G. Ying, C. Crossman, P. Valencia, D. Swain, and G. Bishop-Hurley, "Transforming Agriculture through Pervasive Wireless Sensor Networks," *Pervasive Comput.*, vol.6, no.2, pp.50-57, Apr.-June 2007.
- [2] C. Bauckhage, K. Kersting, and A. Schmidt, "Agriculture's Technological Makeover," *Pervasive Comput.*, vol.11, no.2, pp.4-7, Feb. 2012.
- [3] H. Liu, M. Bolic, A. Nayak, and I. Stojmenovic, "Taxonomy and Challenges of the Integration of RFID and Wireless Sensor Networks," *IEEE Network*, vol.22, no.6, pp.26-35, 2008.
- [4] S. Kim, C. Mariotti, F. Alimenti, P. Mezzanotte, A. Georgiadis, A. Collado, L. Roselli, and M. M. Tentzeris, "No Battery Required: Perpetual RFID-Enabled Wireless Sensors for Cognitive Intelligence Applications," *IEEE Microw. Mag.*, vol.14, no.5, pp.66-77, July 2013.
- [5] R. Want, "Enabling Ubiquitous Sensing with RFID," *Computer*, vol.37, no.4, pp.84-86, Apr. 2004.
- [6] V. Radonic, G. Kitic, and V. Cmojevic-Bengin, "Novel Hilbert soil-moisture sensor based on the phase shift method," *2010 Mediterranean Microwave Symposium (MMS)*, Guzelyurt, Turkey, Aug.2010, pp.377-380.
- [7] S. Kim, B. Cook, T. Le, J. Cooper, H. Lee, V. Lakafosis, R. Vyas, R. Moro, A. Georgiadis, A. Collado, and M. M. Tentzeris, "Inkjet-printed Antennas, Sensors, and Circuits on Paper Substrate," *IET Microw. Antennas Propag.*, vol.7, no.10, pp.858-868, July 2013.
- [8] *Standard Test Method for Laboratory Determination of Water (Moisture) Content of Soil and Rocky by Mass*, ASTM, D2216-98, 1999.